



北京  
应用物理与计算数学研究所  
Institute of Applied Physics  
and Computational Mathematics

**12th International Workshop on  
the Mechanisms of Vacuum Arcs  
(MeVArc 2025)**

# **Three-dimension hybrid simulation on plasma jet formation in Zirconium-Deuterium multi-component vacuum arc discharge**

**Wei Yang, Qiang Sun, Mengmeng Song, Qianhong Zhou**

**yangwei861212@126.com**

**Institute of Applied Physics and Computational Mathematics**

**2025.06**

# Table of contents



**Introduction: vacuum arcs of composite electrode**



**Insights from PIC-DSMC simulations**



**Insights from multi-component fluid simulation**



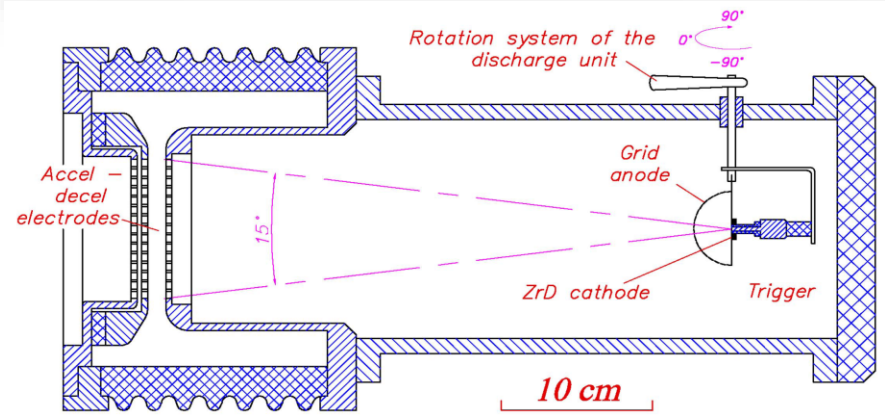
**Recent results of three-dimension hybrid simulation**



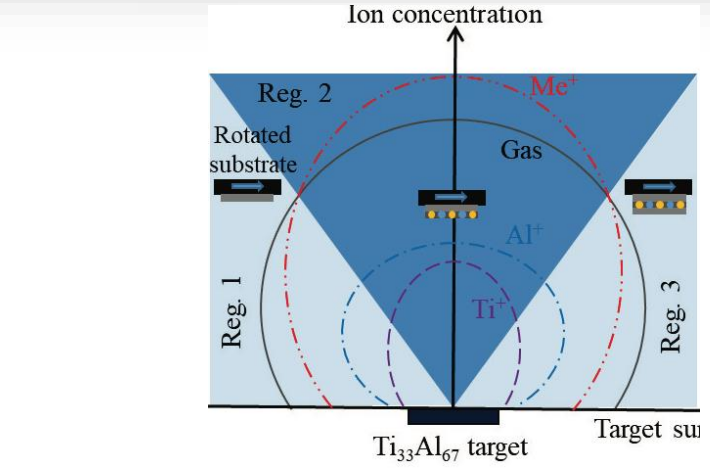
**Conclusions**

# Vacuum arcs of multi-component composite cathode

- Vacuum arcs (VA) of **multi-component composite cathode** have been widely used in ion source, thin film deposition and other industrial fields, due to its **ability to generate ion beams of different elements.**



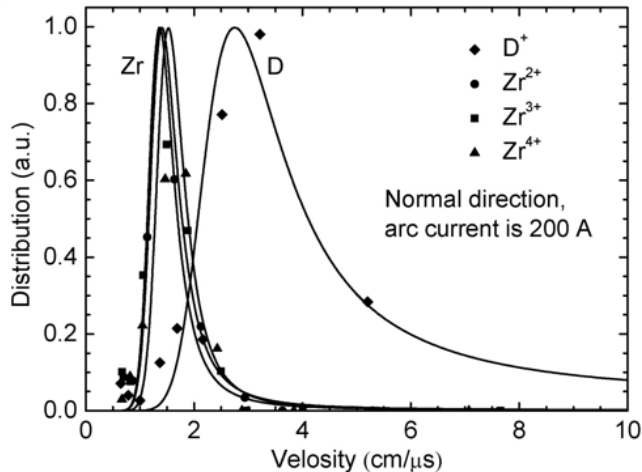
A. G. Nikolaev, *IEEE TPS* **47**, 3590 (2019)



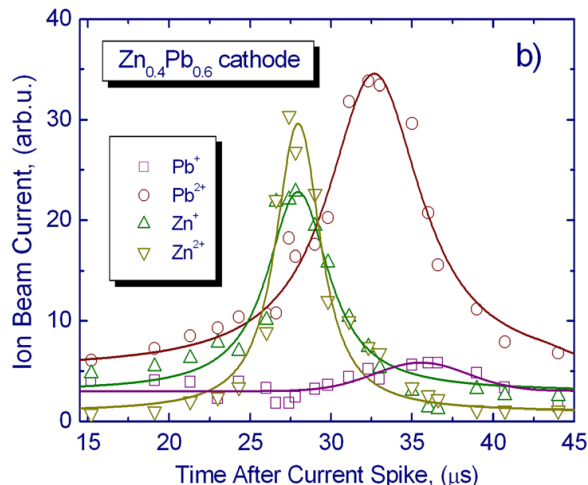
Liu H, et al. *Appl Surf Sci*, **501**, 144025 (2020).

# Velocity distribution of two-component vacuum arcs

- The **directed velocity of light ions** is slightly higher than that of **heavy ions**.
- The directed velocity of ions of **same element but with different charge states** is usually very **close to each other**.



Frolova et al., *28th ISDEIV* (2018).

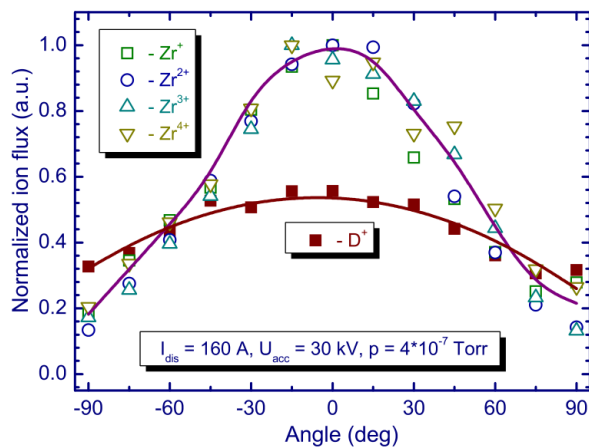


A. G. Nikolaev, *J Appl Phys* **116**, 213303 (2014)

Multicomponent cathode		
Ion	Fraction (%)	Streaming velocity (10 <sup>6</sup> cm/s)
Zn <sup>+</sup>	84	0.82
Zn <sup>2+</sup>	16	0.79
Pb <sup>+</sup>	31	0.62
Pb <sup>2+</sup>	69	0.67

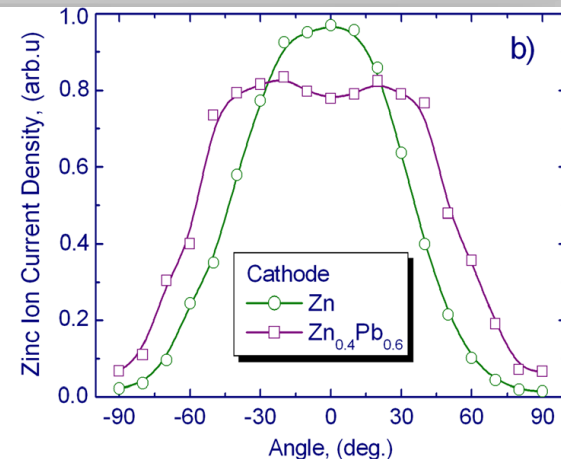
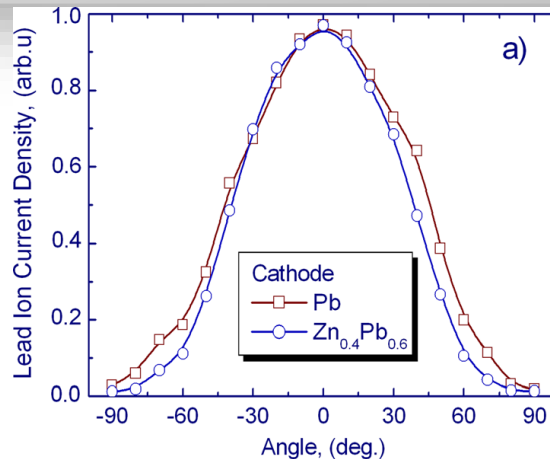
# Angular distribution of two-component vacuum arcs

- The **angular distribution** of light ions is rather uniform, while that of heavy ions is more concentrated in the central axis.
- Comparing the angular distribution of **pure metal cathode and composite cathode**, similar trend is observed for heavy ions but different for light ions.



**Angular distributions of ions (ZrD)**

A. G. Nikolaev, *IEEE TPS* **47**, 3590 (2019).



**comparisons: pure metal cathode and composite cathode**

A. G. Nikolaev, *J Appl Phys* **116**, 213303 (2014)

# Table of contents



**Introduction: vacuum arcs of composite electrode**



**Insights from PIC-DSMC simulations**



**Insights from multi-component fluid simulation**



**Recent results of three-dimension hybrid simulation**

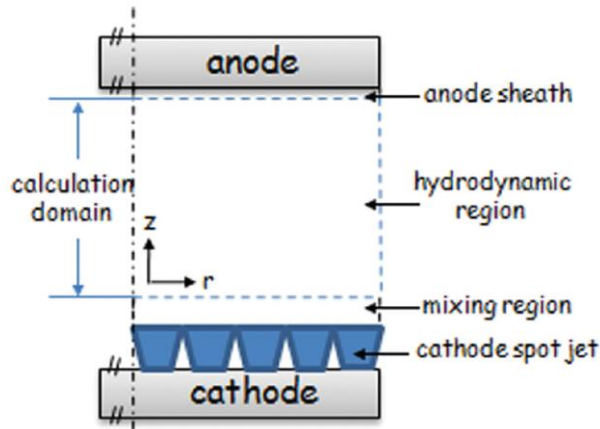


**Conclusions**

# The structure of VA plasma and their parameters

- The vacuum arc plasma is composed of **sheath, cathode spot, plasma jet, arc column** etc., in which physical parameters can vary orders-of-magnitude! Therefore, different numerical approaches are needed.

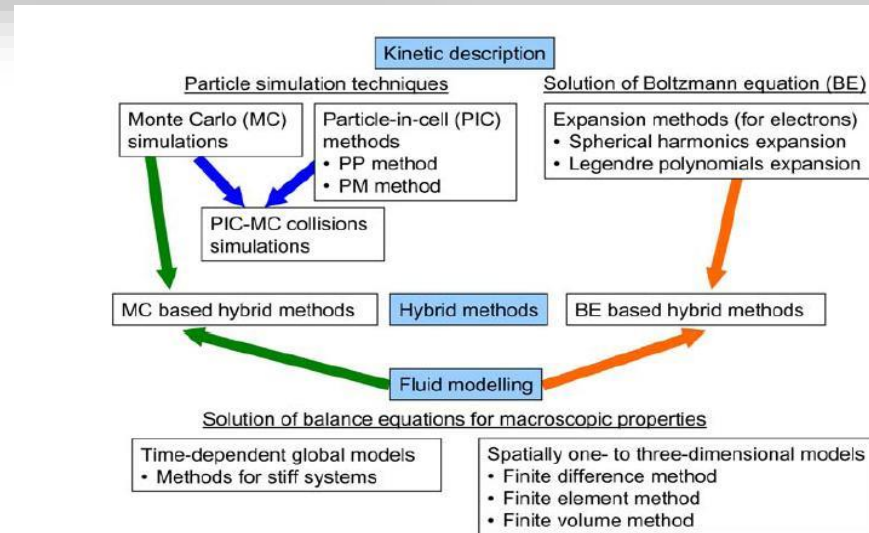
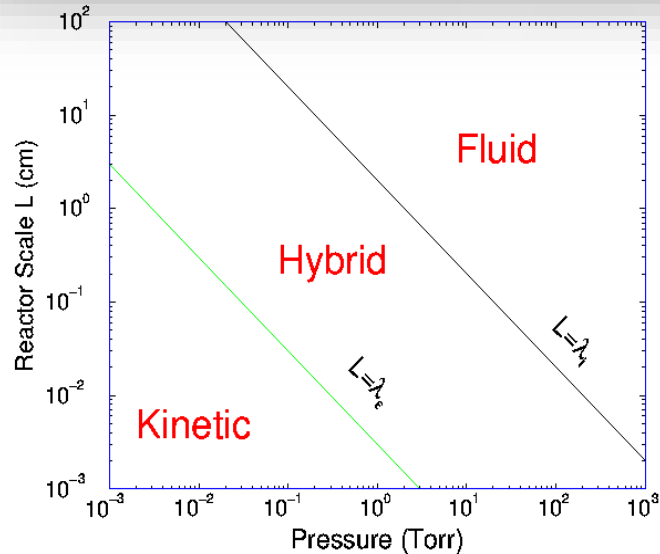
➤ different zone of vacuum arc plasma    ➤ parameters of arc column and cathode spot



	arc column	cathode spot
electric field	$\sim \text{MV/m}$	$> \text{GV/m}$
current density	$10^7 - 10^8 \text{ A/m}^2$	$10^8 - 10^{12} \text{ A/m}^2$
plasma density	$10^{21} - 10^{22} \text{ m}^{-3}$	$10^{20} - 10^{27} \text{ m}^{-3}$
pressure	$\sim 10^3 \text{ Pa}$	$1 \text{ Pa} - 10^7 \text{ Pa}$

# The numerical approaches: kinetic, fluid and hybrid

- The numerical approaches are usually chosen according to **reactor scale** and **mean free path (gas pressure)**, and categorized by the description of (full/partial) kinetic behavior of particle species.



# fully kinetic PIC-DSMC method is computationally heavy

- In standard DSMC simulations, the spatial step should resolve mean free path, time step should resolve collision frequency, and around 100 particles per cell (to avoid stochastic noise).

$$\Delta x < \lambda_{\text{MFP}} \quad \Delta t < 0.1 / \nu_{\text{collision}} \quad \text{PPC (particles per cell)} \sim 100$$

- In **explicit** ES-PIC simulations, the spatial step should resolve Debye length (to avoid numerical heating), and time step should resolve plasma oscillation frequency.

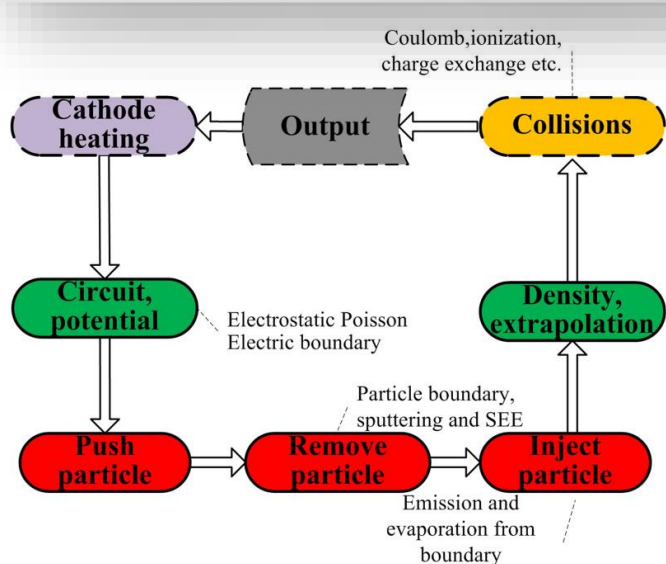
$$\Delta x < 3.4 \lambda_D \quad \Delta t < 0.2 / \omega_{pe}$$

- Although **implicit** scheme can enlarge the temporal step, the **Courant–Friedrichs–Lewy (CFL)** condition should always be ensured (particles do not travel across spatial cell per step).

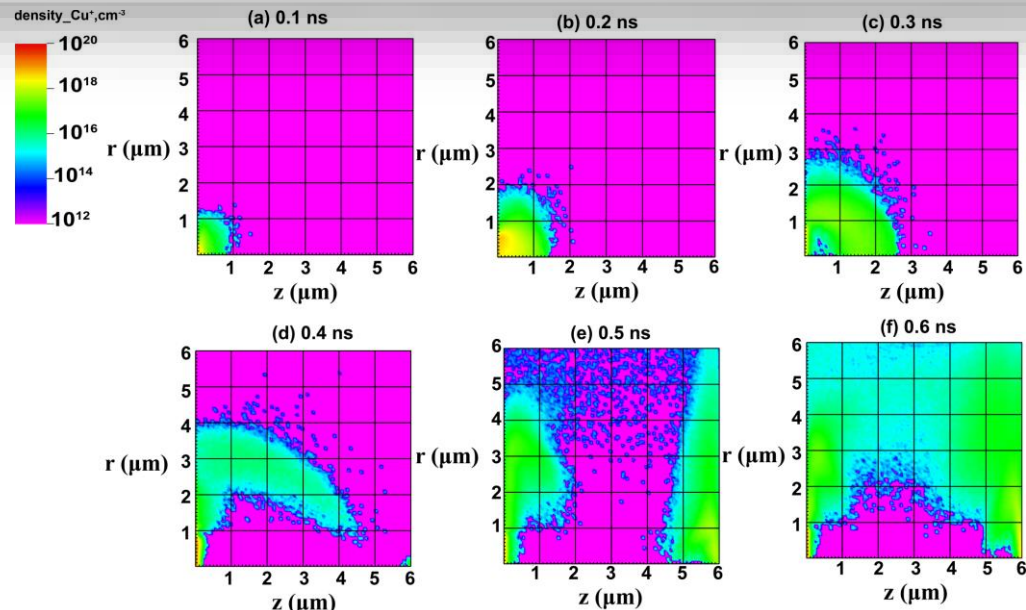
$$\Delta t < \Delta x / v_{te} \quad \omega_{pe} = \sqrt{\frac{e^2 n_e}{\epsilon_0 m_e}} = v_{te} / \lambda_{DB}$$

# Fully kinetic 2D modeling on short-gap vacuum breakdown

- Previously, a **2D r-z geometry electrostatic (ES) PIC-DSMC** fully kinetic model is used to simulate **micro-meters scale** short-gap vacuum breakdown.



The computing cycle of PIC-DSMC simulation at each time step



$\text{Cu}^+$  density distribution at different times during the short-gap vacuum breakdown

# 1D3V spherical PIC-DSMC method: time-saving technique

- **Time-saving technique: effective cross-section method for Coulomb collision**

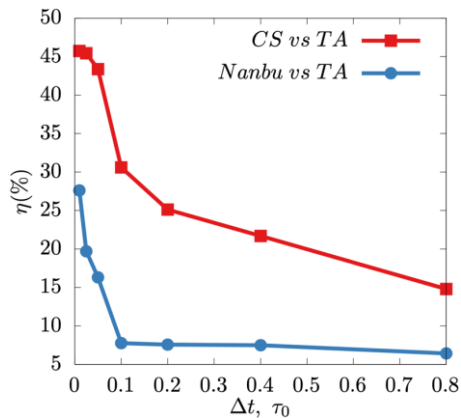
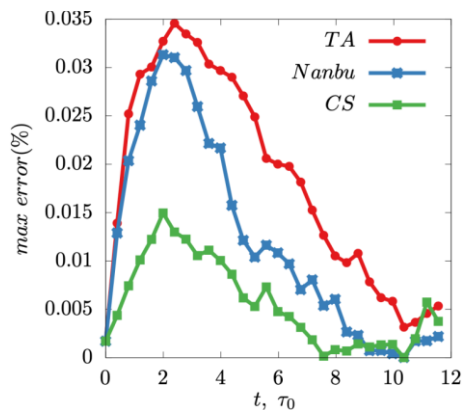
$$P_c = 1 - \exp(-\sigma_m n_\beta u \Delta t), \quad \sigma_m = 16\pi b_0^2 \ln \Lambda$$

- **Time-saving technique: 1D spherical momentum-conserving implicit PIC scheme**

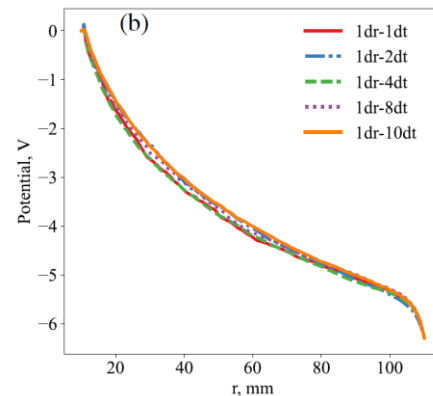
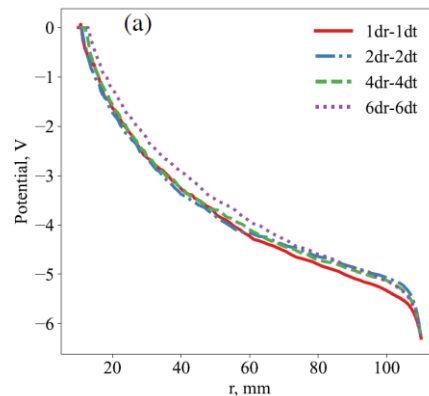
$$v^{n+\frac{1}{2}} = v^{n-\frac{1}{2}} + \frac{(\bar{a}^{n-1} + a^{n+1}) \Delta t}{2}, \quad r^{n+1} = r^n + v^{n+\frac{1}{2}} \Delta t$$

$$a^{n+1} = \frac{q}{m} E^{n+1} + \left( \frac{v_\theta^2 + v_\varphi^2}{r} \right)^{n+1}$$

$$\nabla \cdot [\varepsilon_0 (1 + \chi) \nabla \phi^{n+1}] - \nabla \cdot \left[ \frac{1}{2} \left( \frac{v_\theta^2 + v_\varphi^2}{r} \right)^{n+1} \Delta t^2 \bar{\rho}^{n+1} \right] = -\bar{\rho}^{n+1}$$



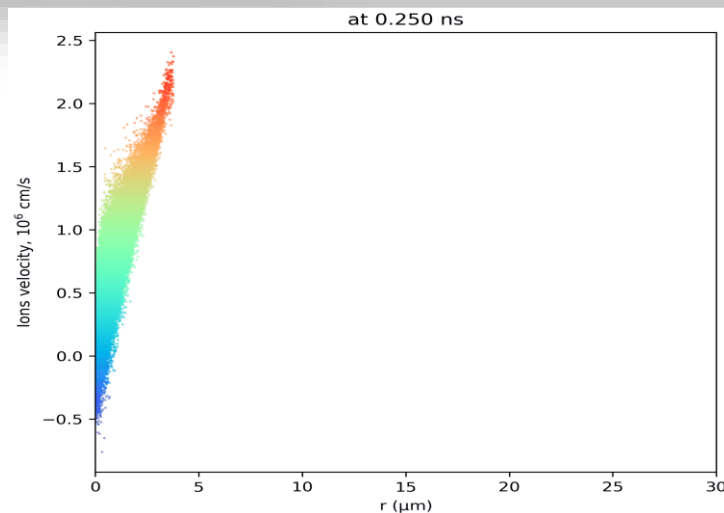
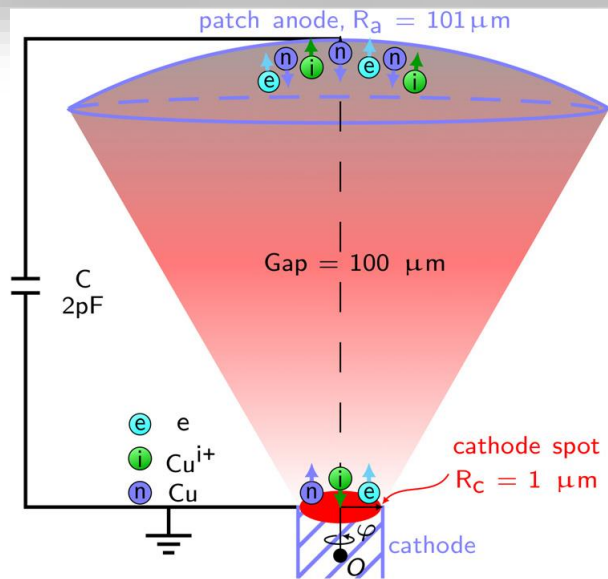
**comparison with traditional TA and Nanbu method: accuracy and improved efficiency**



**Implicit scheme with larger spatial and time steps compared with explicit scheme: 1dr1dt**

# 1D spherical PIC-DSMC simulation on plasma expansion

- 1D spherical PIC-DSMC method was used to study ion acceleration in vacuum spark and arcs, VA plasmas of composite cathode in longer gaps ( **$\sim 100$  microns**)



plasma expansion in quasi-spherical geometry

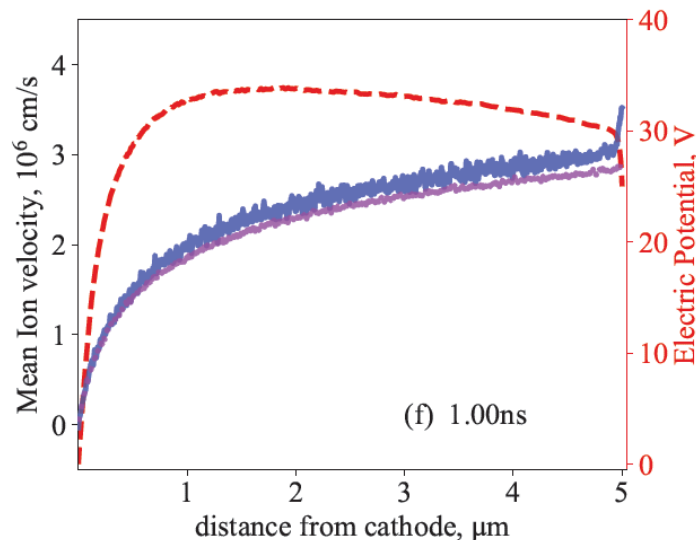
Phase-space plot showing ion acceleration

Song et al., *Phys Plasmas*, **32**, 023506, 2025; *J Phys D: Appl Phys*, **57**, 315207, 2024

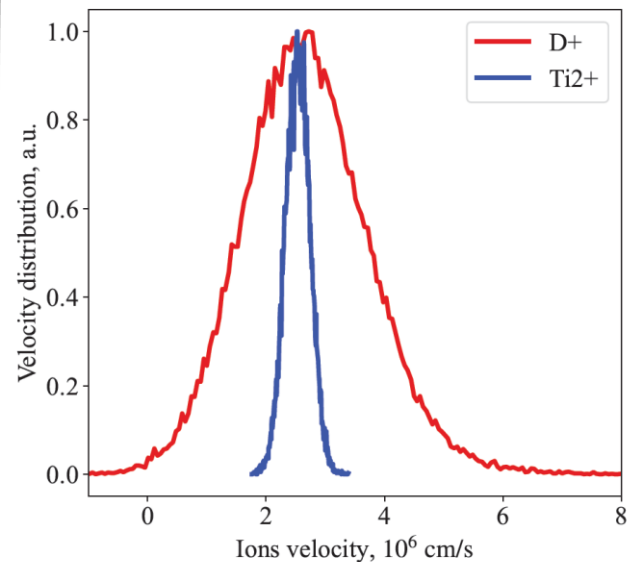
*Plasma Source Sci Technol*, **33**, 105009, 2024; *Plasma Source Sci Technol*, **32**, 095002, 2023

# Insights from 1D3V PIC simulation

- The directed velocity of light and heavy ions is quite close. However, light ions show higher thermal velocity. These effects make the expansion of D ions more isotropically in broad area (thermal energy->kinetic energy), but is not affordable in PIC simulation (mm-scale).



The directed velocity of ions (solid line)  
as well as potential distribution (red dash)

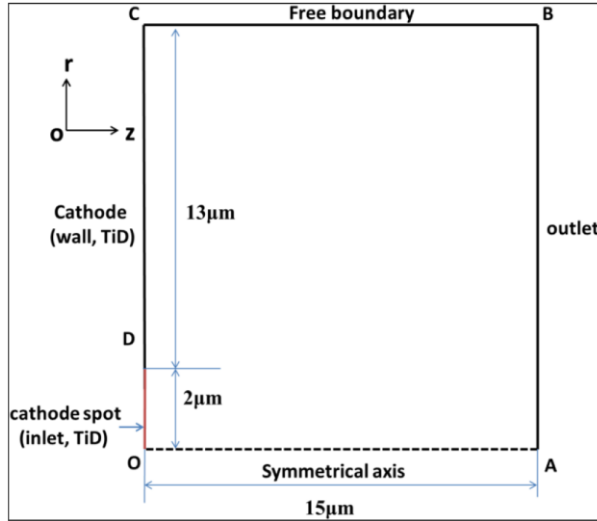


Ion velocity distribution

# Table of contents

**I****Introduction: vacuum arcs of composite electrode****II****Insights from PIC-DSMC simulations****III****Insights from multi-component fluid simulation****IV****Recent results of three-dimension hybrid simulation****V****Conclusions**

# Simulation domain, assumptions and BCs of fluid model 15

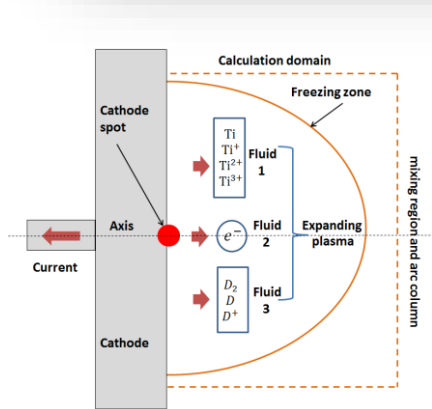


1. The system is assumed to be **2D axisymmetric** and in **steady state**.
2. Each species (for example Ti, Ti<sup>+</sup>, Ti<sup>2+</sup>, Ti<sup>3+</sup>) has the same velocity and temperature.
3. The plasma is assumed to be **quasi-neutral**.
4. The electron inertia and viscosity can be neglected.
5. the Lorentz forces can be ignored compared to the pressure gradients.
6. The electrons and ions are regarded as ideal gases.

Boundary	$T_e$	$\varphi$	$n_i$	$u_i$	$T_i$	$n_d$	$u_d$	$T_d$
A–B–C (outlet)	$\frac{\partial T_e}{\partial n} = 0$	$\varphi = 0$	—	Supersonic	—	—	Supersonic	—
C–D (wall)	1.5 eV	$\frac{\partial \varphi}{\partial n} = 0$	—	—	3000 K	—	—	3000 K
D–O (inlet)	1.5 eV	$j$	$f_{Ti}$	Subsonic	8000 K	$f_D$	Subsonic	8000 K
O–A (axis)	$\frac{\partial T_e}{\partial n} = 0$	$\frac{\partial \varphi}{\partial n} = 0$	$\frac{\partial n_i}{\partial n} = 0$	$\frac{\partial u_i}{\partial n} = 0$	$\frac{\partial T_i}{\partial n} = 0$	$\frac{\partial n_d}{\partial n} = 0$	$\frac{\partial u_d}{\partial n} = 0$	$\frac{\partial T_d}{\partial n} = 0$

# Fluid model of multi-component plasma jet

- To study the physical process of a cathode spot jet in VA with metal deuteride cathode (TiD), a two-dimensional hydrodynamic model based on three-fluid theory is established.
- 28 reaction channels with 8 plasma species are considered, including ionization and recombination processes.



collision particle	collision type	Reaction
e, D <sub>2</sub> /D/Ti	Dissociation	$e + D_2 \rightarrow e + 2D$
	Elastic collision	$e + D_2/D/Ti \rightarrow e + 2D$
	Excitation	$e + D \rightarrow e + D^*$
	Ionization	$e + D/Ti \rightarrow 2e + D^+/Ti^+$
e, D <sup>*</sup>	Ionization	$e + D^* \rightarrow 2e + D^+$
e, D <sup>+</sup> /Ti <sup>n+</sup>	Cascade ionization	$e + Ti^{n+} \rightarrow 2e + Ti^{(n+1)+}$
	recombination	$e + e + D^+/Ti^+ \rightarrow e + D/Ti$ $e + e + Ti^{n+} \rightarrow e + Ti^{(n-1)+}$
D <sub>2</sub> /D/D <sup>+</sup> Ti/Ti <sup>n+</sup>	Elastic collision	$D_2/D + Ti/Ti^{n+} \rightarrow D_2/D + Ti/Ti^{n+}$ $Ti + D_2/D/D^+ \rightarrow Ti + D_2/D/D^+$
	Coulomb collision	$D^+ + Ti^{n+} \rightarrow D^+ + Ti^{n+}$

$$\begin{aligned}
 & \nabla \cdot (n_i \mathbf{u}_i) = 0 & 1 \\
 & m_i n_i (\mathbf{u}_i \cdot \nabla) \mathbf{u}_i = -\nabla p_i - \frac{Z_i n_i}{n_e} \nabla p_e + \nabla \cdot \bar{\tau}_i & 2 \\
 & + (n_e - Z_i n_i) m_e v_{ei} (\mathbf{u}_e - \mathbf{u}_i) - Z_i n_i m_e v_{ei} (\mathbf{u}_e - \mathbf{u}_d) + n_d m_d v_{di} (\mathbf{u}_d - \mathbf{u}_i) & \\
 & \frac{3}{2} n_i k (\mathbf{u}_i \cdot \nabla T_i) + p_i \nabla \cdot (\mathbf{u}_i) = \nabla \cdot (\lambda_i \nabla T_i) + \frac{3k m_e n_e v_{ei}}{m_i} (T_e - T_i) + \frac{3k m_d n_d v_{di}}{m_i} (T_d - T_i) + \bar{\tau}_i \cdot \nabla (\mathbf{u}_i) & 3 \\
 & \nabla \cdot (\rho_i \mathbf{u}_i c_{ij} + \mathbf{J}_E) = S_{ij} & 4 \\
 & \nabla \cdot (n_d \mathbf{u}_d) = 0 & 5 \\
 & m_d n_d (\mathbf{u}_d \cdot \nabla) \mathbf{u}_d = -\nabla p_d - \frac{n_d}{n_e} \nabla p_e + \nabla \cdot \bar{\tau}_d & 6 \\
 & + (n_e - n_d) m_e v_{ed} (\mathbf{u}_e - \mathbf{u}_d) - n_d m_e v_{ei} (\mathbf{u}_e - \mathbf{u}_i) - n_d m_d v_{di} (\mathbf{u}_d - \mathbf{u}_i) & \\
 & \frac{3}{2} n_d k (\mathbf{u}_d \cdot \nabla T_d) + p_d \nabla \cdot (\mathbf{u}_d) = \nabla \cdot (\lambda_d \nabla T_d) + \frac{3k m_e n_e v_{ed}}{m_d} (T_e - T_d) - \frac{3k m_d n_d v_{di}}{m_i} (T_d - T_i) + \bar{\tau}_d \cdot \nabla (\mathbf{u}_d) & 7 \\
 & \nabla \cdot (\rho_d \mathbf{u}_d c_{dj} + \mathbf{J}_E) = S_{dj} & 8 \\
 & \frac{3}{2} n_e k (\mathbf{u}_e \cdot \nabla T_e) + p_e \nabla \cdot (\mathbf{u}_e) = \nabla \cdot (\lambda_e \nabla T_e) - \frac{3k m_e n_e v_{ei}}{m_i} (T_e - T_i) - \frac{3k m_e n_e v_{ed}}{m_d} (T_e - T_d) + \frac{j^2}{\sigma} - U_{ioniz} & 9 \\
 & \nabla \cdot \mathbf{j} = 0 & 10 \\
 & n_e = Z_i n_i + n_d, \quad \mathbf{u}_e = (Z_i n_i \mathbf{u}_i + n_d \mathbf{u}_d - \mathbf{j}/e)/n_e & 11
 \end{aligned}$$

Labels on the right side of the equations: metal ion (1-3), Deuterium ion (4-7), Electron (8-11).

schematic of fluid model

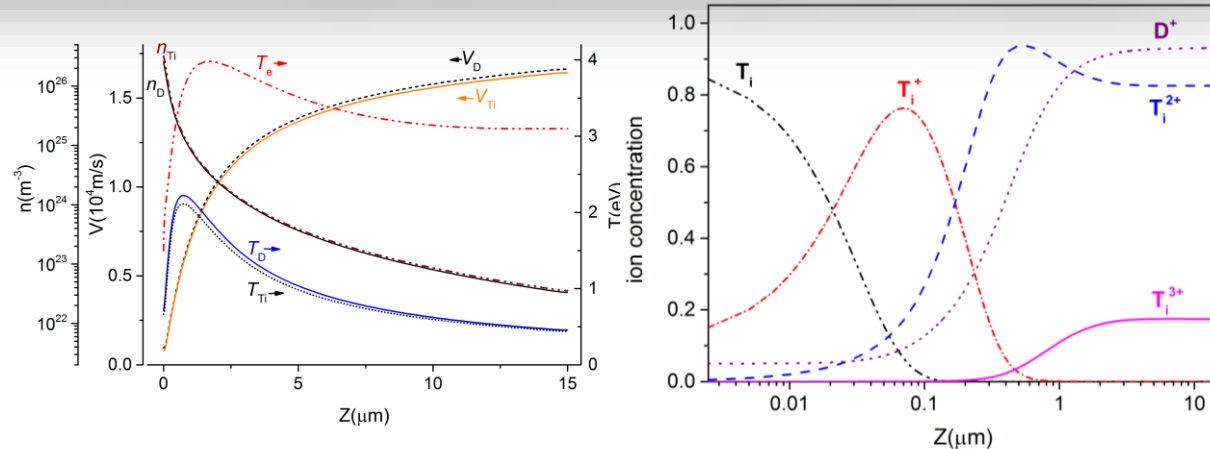
28 reaction channels

governing equations in steady state

# calculated plasma parameters and comparison with experiment

- The charge states and directed velocity of metal ions agreed well with previous experiment.
- However, the **directed velocity of light and heavy ions is quite close in simulation.**

calculated plasma parameters along the z axis



comparison with experimental results in literature

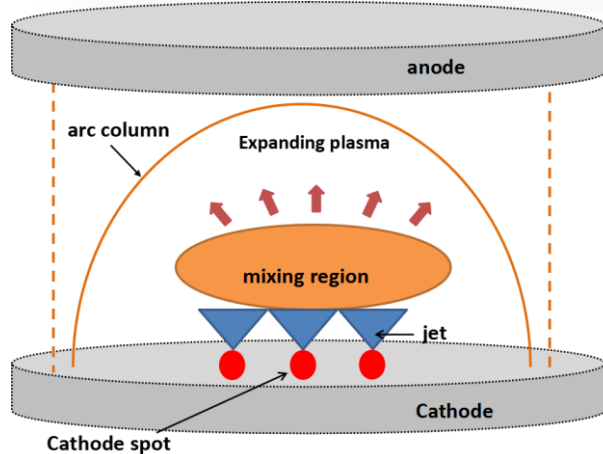
Plasma parameter	Simulation results	Experimental results
$Z_i$	2.03-2.33	2.0-2.3 [1]
$V_i$	16320m/s	15400m/s [2]
$Ma$	4.43	4.3 [2]

[1] Oks E M, Anders A, Brown I, Dickinson M and MacGill R 1996 *IEEE TPS* **24** 1174

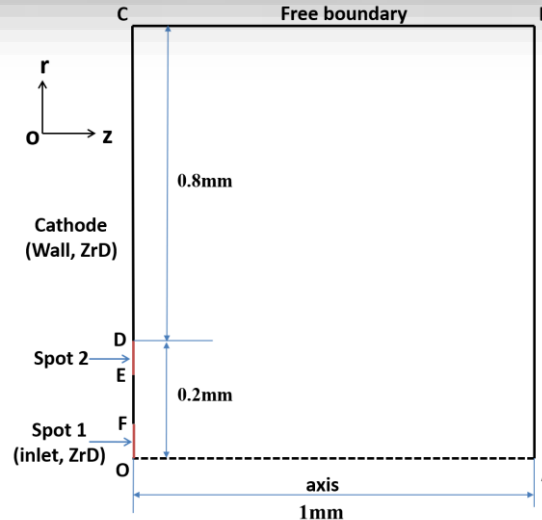
[2] Anders A and Yushkov G Y 2002 *JAP* **91** 4824

# plasma jet mixing of multi-component VA plasma

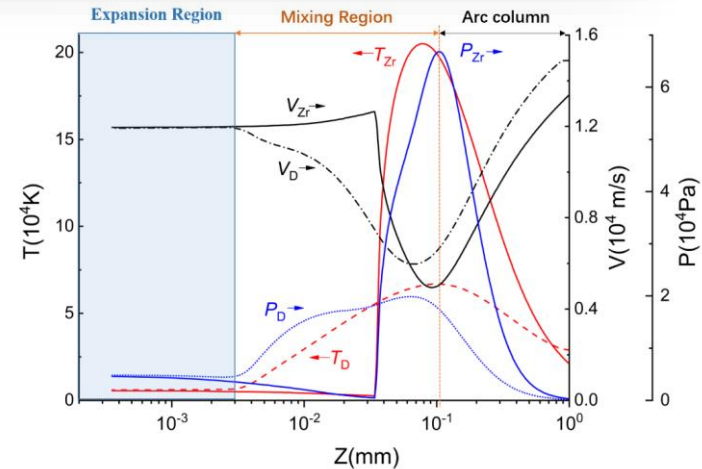
- While directed velocity of light and heavy ions is close in plasma expansion of single cathode spot (CS), the **plasma jet mixing of multiply CS** is simulated in **mm-scale**.
- Due to 2D r-z geometry, two CS is set in the inlet: the **spot 1** has a circular shape but the **spot 2** has a ring shape, representing a number of separate CS.



schematic of jet mixing

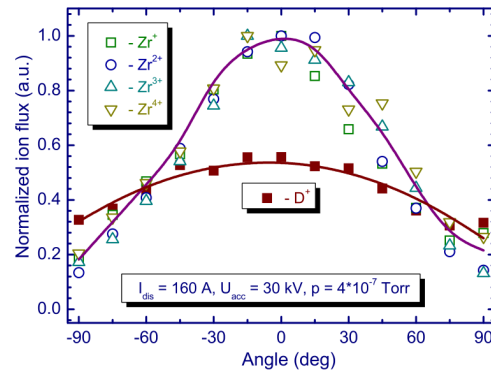
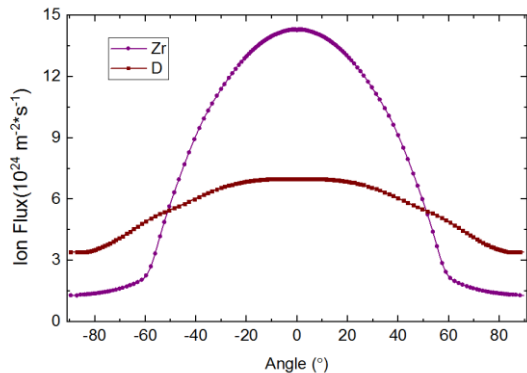


simulation domain with two CS



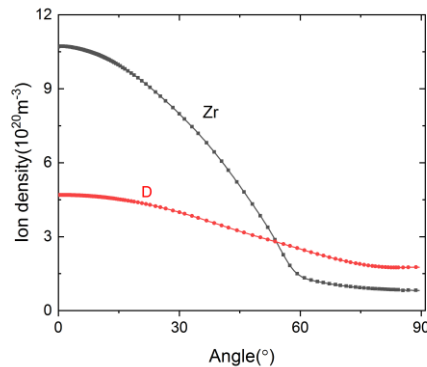
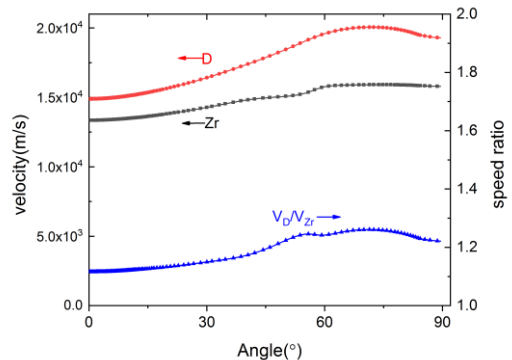
velocity separation in arc column

# velocity and flux separation of light and heavy ions



angular distribution of **ion flux**: simulation

angular distribution of **ion flux**: experiment\*



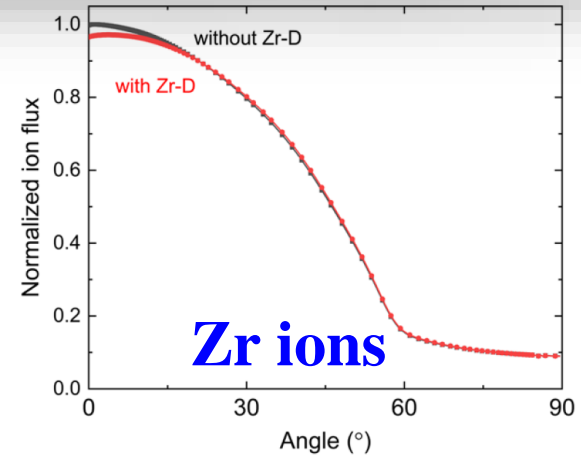
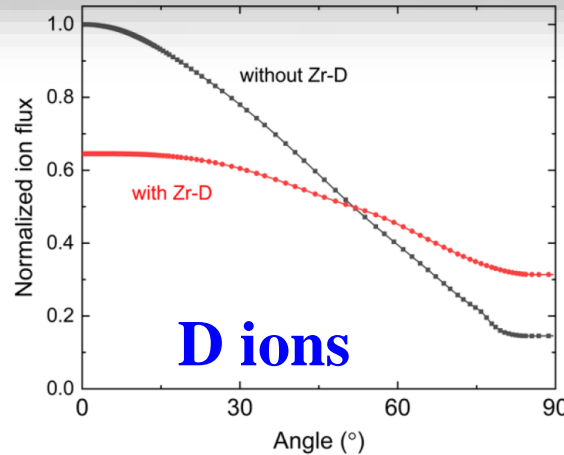
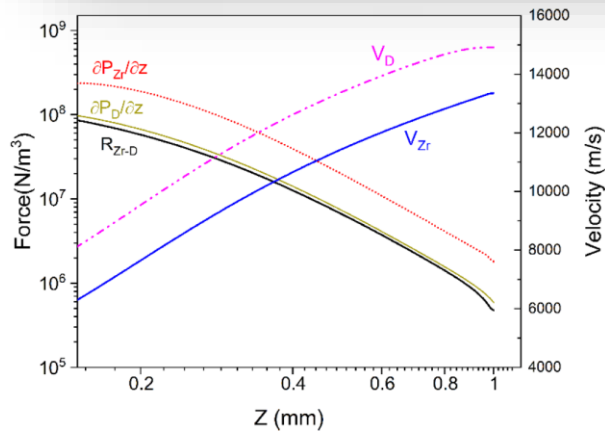
angular distribution of **ion velocity**: simulation

angular distribution of **ion density**: simulation

\* Nikolaev A G 2019 *IEEE Trans. Plasma Sci.* **47** 3590

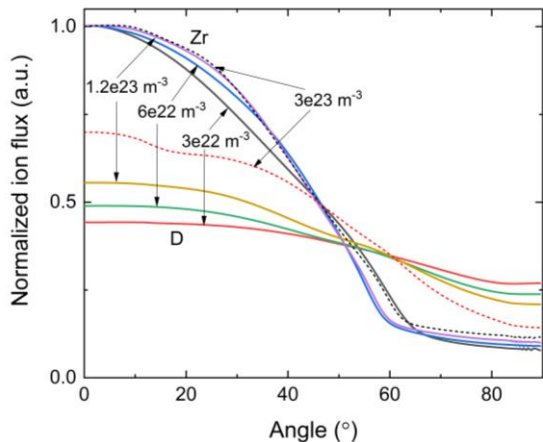
# The underline mechanism: collision between D-Zr ions

- **Zr–D ion collision force  $R_{Zr-D}$**  is close to the pressure gradient of D, but far less than that of Zr. Therefore,  $R_{Zr-D}$  has **little effect on Zr ions momentum**, but **significant effect on D ions**.
- Comparing the situation **whether the Zr–D ion collision is considered in the model**, the **angular distribution of D ions differs substantially**, but that of Zr ion is similar (*in experiment, angular distribution of heavy ions is similar for pure metal cathode and composite cathode*).

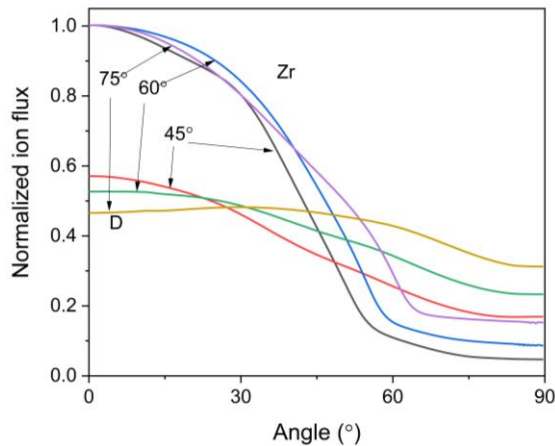


**collision term v.s. pressure gradient**    **The ion flux angular distribution with and without Zr–D collisions**

# The influencing factors: ion density, temperature and mass



The influence of ion density



The influence of ion temperature  
(via incident angle)



The influence of ion mass

- The separation of ions can be enhanced by increasing ion temperature, decreasing ion density and selecting electrode components with significant differences in elemental mass.

$$R_{d-i} = n_d m_d v_{di} (u_d - u_i) \quad v_{di} = \left( \frac{m_e}{m_d} \right)^{1/2} \cdot \left( \frac{T_e}{T_d} \right)^{3/2} \cdot v_{ei}, \quad v_{ei} = \frac{Z_i^2 n_i (\ln \Lambda / 10)}{3.5 \times 10^{10} (T_e [\text{eV}])^{3/2}}$$

# Table of contents

**I****Introduction: vacuum arcs of composite electrode****II****Insights from PIC-DSMC simulations****III****Insights from multi-component fluid simulation****IV****Recent results of three-dimension hybrid simulation****V****Conclusions**

# Hybrid model of multi-component plasma jets

- Ions are treated as super-particles, and ion kinetics are tracked.
- Electrons are treated as mass-less fluids, and electron kinetics is not

resolved. PIC module  
(ions: velocity  $v_i$  and position  $x_i$ )

fluid module  
(electrons: density, velocity, and temperature)

assumption 1: quasi-neutrality  
assumption 2: mass-less fluid

Electromagnetic field module  
(electric field  $E$  and magnetic field  $B$ )

Darwin approximation

$$\frac{dx_i}{dt} = v_i$$

$$m_i \frac{dv_i}{dt} = q_i (\mathbf{E} + \mathbf{v}_i \times \mathbf{B}) - \mathbf{f}$$

$$n_e = q_i n_i$$

$$n_e m_e \frac{dv_e}{dt} = \mathbf{0} = -en_e (\mathbf{E} + \mathbf{v}_e \times \mathbf{B}) - \nabla p_e + \frac{en_e \mathbf{j}}{\sigma}$$

$$\frac{\partial (\frac{3}{2} n_e k T_e)}{\partial t} + \frac{3}{2} n_e k \mathbf{u}_e \cdot \nabla T_e + p_e (\nabla \cdot \mathbf{u}_e) = \nabla \cdot (k_e \nabla T_e) + \frac{j^2}{\sigma} - Q_{ei}$$

$$\frac{\partial \mathbf{B}}{\partial t} = -\nabla \times \mathbf{E}$$

$$\mathbf{0} = \frac{1}{\mu_0} \nabla \times \mathbf{B} - \mathbf{j}$$

# Pros and cons of Darwin approximation in hybrid model <sup>24</sup>

## Maxwell equation

$$\frac{\partial \mathbf{B}}{\partial t} = -\nabla \times \mathbf{E}$$
$$\epsilon_0 \frac{\partial \mathbf{E}}{\partial t} = \frac{1}{\mu_0} \nabla \times \mathbf{B} - \mathbf{j}$$

## Darwin approximation

$$\frac{\partial \mathbf{B}}{\partial t} = -\nabla \times \mathbf{E}$$
$$0 = \frac{1}{\mu_0} \nabla \times \mathbf{B} - \mathbf{j}$$

## generalized Ohm's law: different forms

$$\mathbf{j} = \sigma \left( \mathbf{E} + \mathbf{v}_e \times \mathbf{B} + \frac{\nabla p_e}{en_e} \right)$$

$$\mathbf{E} = -\mathbf{v}_e \times \mathbf{B} - \frac{\nabla p_e}{en_e} + \frac{\mathbf{j}}{\sigma}$$

## Pros

self-consistent treatment of the electromagnetic field, allowing electromagnetic waves to propagate in vacuum or plasma

## CONS

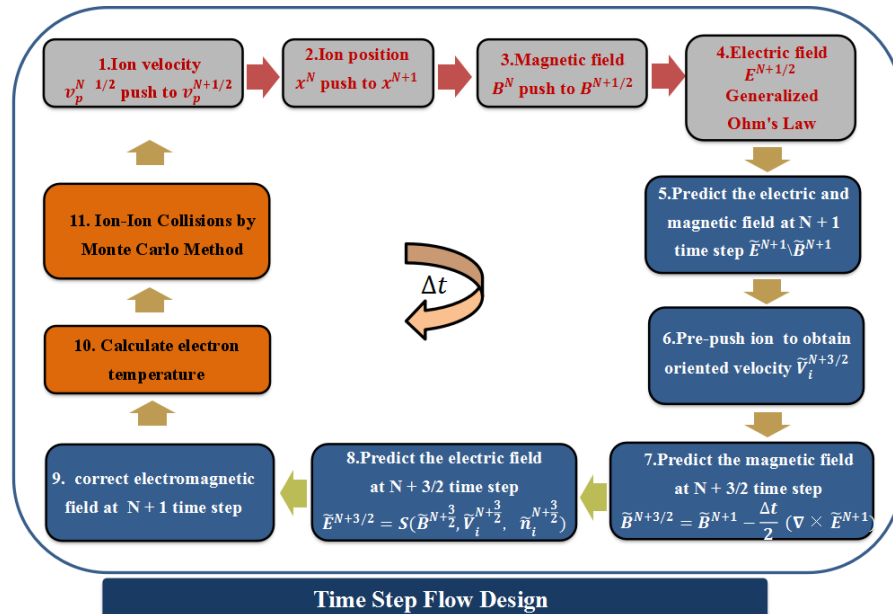
In FDTD scheme, the time step size is strictly limited by the speed of light

Fast calculation, low-frequency approximation, ignoring light waves, only need to deal with ion time scales

the transmission of magnetic field in low density or vacuum region is greatly limited

# predictor-corrector method for high accuracy field solution

- ion position  $x_i^N$  and electric field  $E^N$  are defined on **integer time step**
- ion velocity  $v_i^{N+1/2}$ , magnetic field  $B^{N+1/2}$  and electron fluid variables ( $n_e^{N+1/2}$ ,  $v_e^{N+1/2}$ ,  $T_e^{N+1/2}$ ) are defined on **half integer time step**.
- field is updated by **predictor-corrector method** instead of 1st-order forward Euler



D. Winske, Homa Karimabadi, Ari Le, N. Omidi, Vadim Roytershteyn, Adam Stanier. 2022. Hybrid codes (massless electron fluid)

# methods for electron-ion and ion-ion collision

## □ electron-ion collision by fluid method

In ion pushing, electron-ion friction force is treated

$$\frac{dx_i}{dt} = v_i$$

$$m_i \frac{dv_i}{dt} = q_i (\mathbf{E} + \mathbf{v}_i \times \mathbf{B}) - f$$

friction force is calculated according to the velocity of electrons and ions

$$\text{for Zr: } f = \frac{Z_i (\ln \Lambda / 10)}{3.5 \times 10^{10} [T_e (\text{eV})]^{3/2}} m_e n_e (\mathbf{V}_{Zr} - \mathbf{V}_e)$$

$$\text{for D: } f = \frac{(\ln \Lambda / 10)}{3.5 \times 10^{10} [T_e (\text{eV})]^{3/2}} m_e n_e (\mathbf{V}_D - \mathbf{V}_e)$$

## □ ion-ion collision by Monte-Carlo method

Post-collision velocity is related to pre-collision velocity according to momentum and energy conservation

$$\vec{v}'_{\alpha} = \vec{v}_{\alpha} + \frac{m_{\beta}}{m_{\alpha} + m_{\beta}} \Delta \vec{u}$$

$$\vec{v}'_{\beta} = \vec{v}_{\beta} - \frac{m_{\alpha}}{m_{\alpha} + m_{\beta}} \Delta \vec{u}$$

Based on scattering angle and azimuthal angle sampled in Monte-Carlo method, the relative velocity is calculated.

$$\Delta u_x = (u_x^t / u_{\perp}^t) u_z^t \sin \Theta \cos \Phi - (u_y^t / u_{\perp}^t) u \sin \Theta \sin \Phi - u_x^t (1 - \cos \Theta)$$

$$\Delta u_y = (u_y^t / u_{\perp}^t) u_z^t \sin \Theta \cos \Phi + (u_x^t / u_{\perp}^t) u \sin \Theta \sin \Phi - u_y^t (1 - \cos \Theta)$$

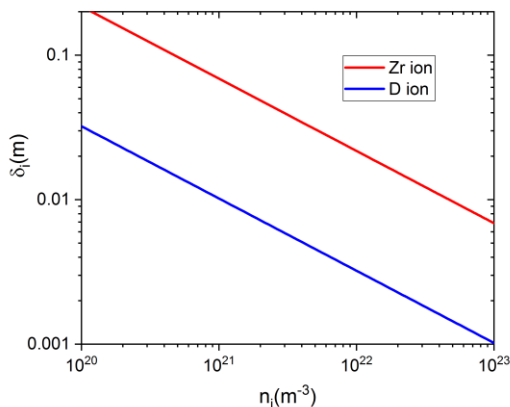
$$\Delta u_z = -u_{\perp}^t \sin \Theta \cos \Phi - u_z^t (1 - \cos \Theta)$$

# constraint on spatial step in hybrid simulation with collision

the minimum of inertial length and mean free path of ions

ion inertial length

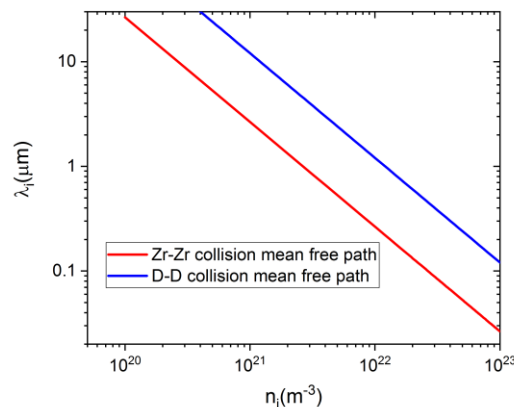
$$\delta_i = \frac{c}{w_{ip}} \quad w_{ip} = \sqrt{\frac{n_i q_i^2}{\epsilon_0 m_i}}$$



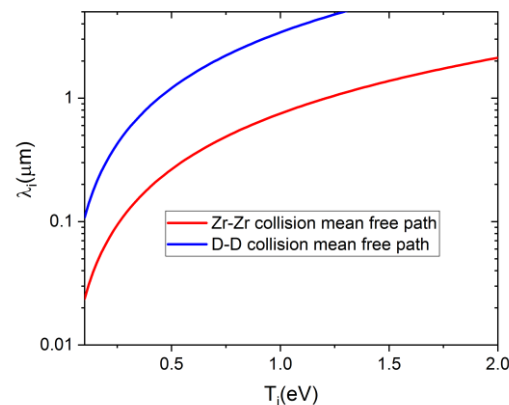
$$\frac{\delta_i}{\lambda_D} = \frac{c}{v_{i,sound}}$$

mean free path of ion-ion collision

$$\lambda_{ii} = \frac{v_i}{v_{ii}} \quad v_{ii} = \frac{n_i Z_i^4 e^4 \ln \Lambda}{12 \pi^{3/2} \epsilon_0^2 m_i^{1/2} (kT_i)^{3/2}}$$



$$\frac{\lambda_{ii}}{\lambda_D} = \frac{2N_D}{Z_i^4} \left(\frac{T_i}{T_e}\right)^{3/2}$$

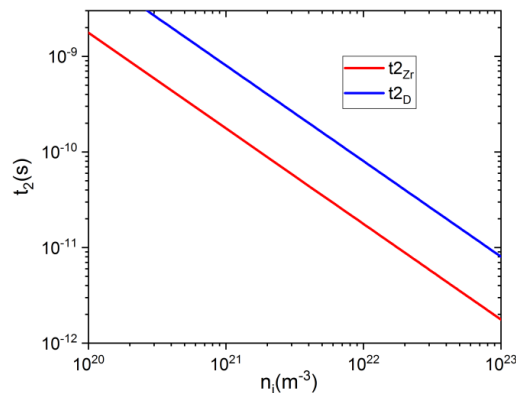
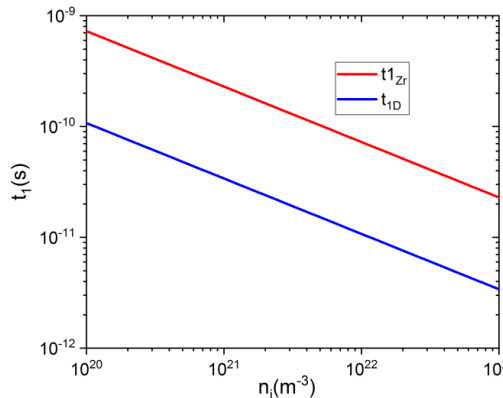


# constraint on time step in hybrid simulation with collision

## ion plasma frequency

$$\Delta t_1 \cdot \omega_{ip} < 1$$

$$\omega_{ip} = \sqrt{\frac{n_i q_i^2}{\epsilon_0 m_i}}$$



## ion collision frequency

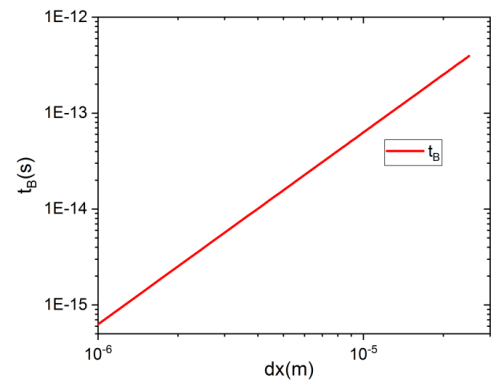
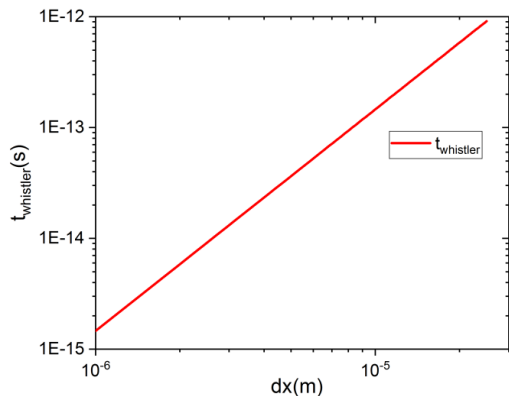
$$\Delta t_2 \cdot \nu_{ii} < 1$$

$$\nu_{ii} = \frac{n_i Z_i^4 e^4 \ln \Lambda}{12 \pi^{3/2} \epsilon_0^2 m_i^{1/2} (k T_i)^{3/2}}$$

## CFL stability criterion for waves in the whistler limit

$$\Delta t < \Delta t_{whistler} = \frac{\omega_i^{-1}}{\pi \sqrt{N}} \left( \frac{\Delta x}{\delta_i} \right)^2$$

$$\Delta t_{whistler} \approx 8.76 \times 10^{-26} \cdot \frac{(\Delta x)^2}{B} \cdot n_i$$

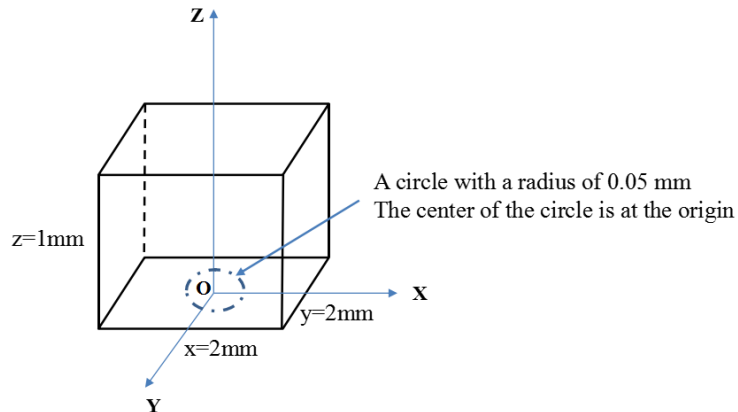
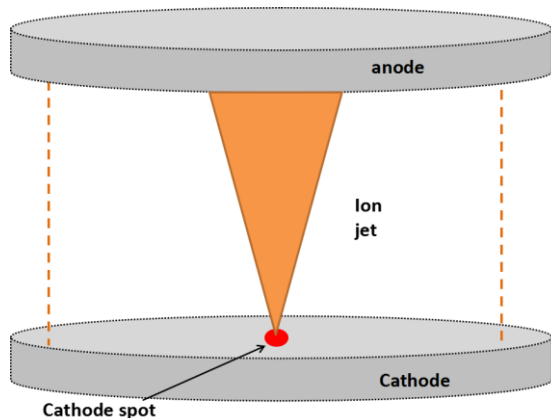


## resistive term of magnetic diffusion equation

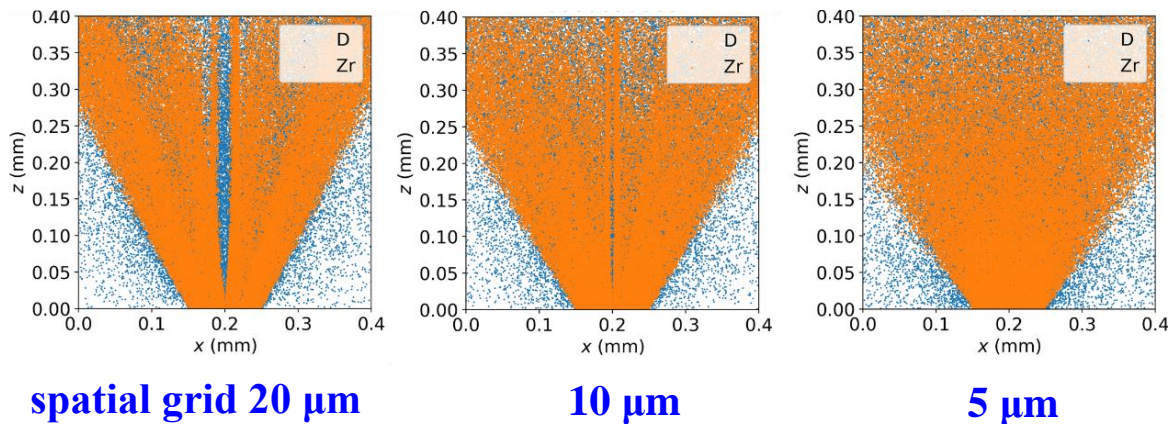
$$\frac{\partial B}{\partial t} = \frac{\eta}{\mu_0} \nabla^2 B$$

$$\Delta t_B < 0.5 \frac{(\Delta x)^2}{\eta / \mu_0}$$

# plasma expansion of single CS: influence of spatial grid

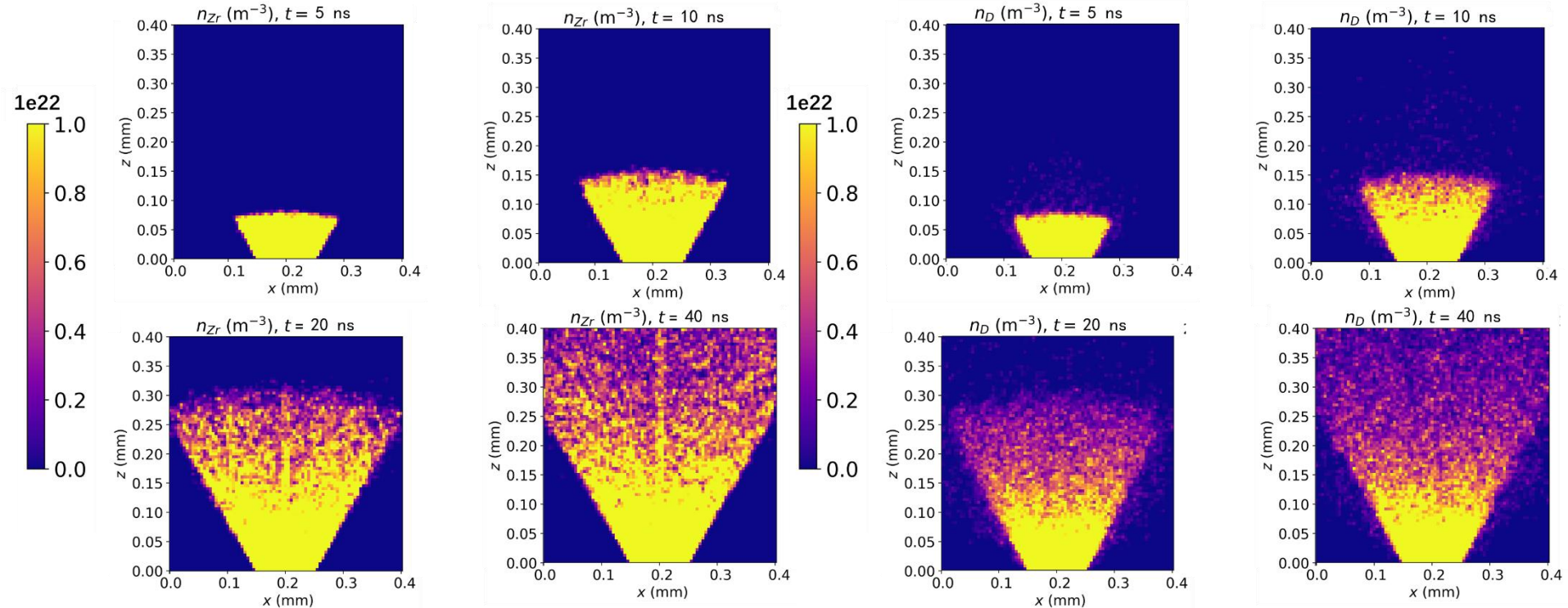


## Schematic of three-dimension hybrid simulation on plasma expansion of single CS



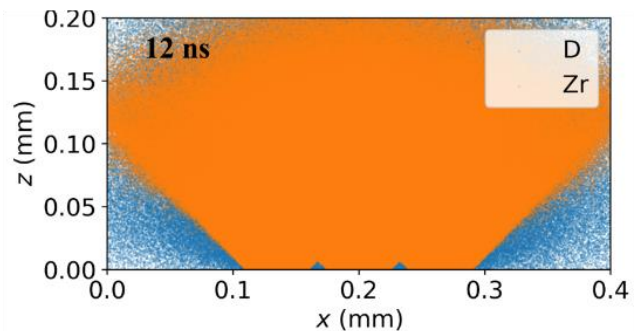
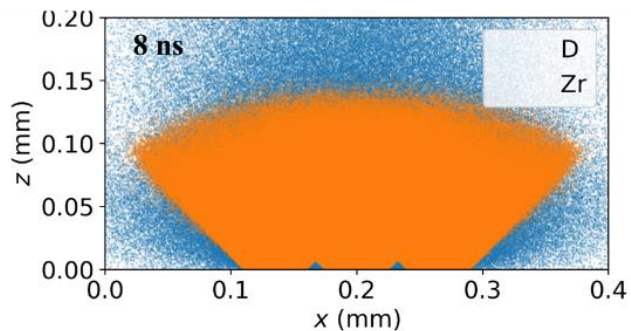
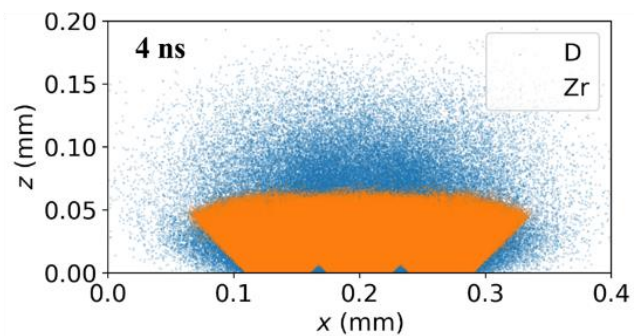
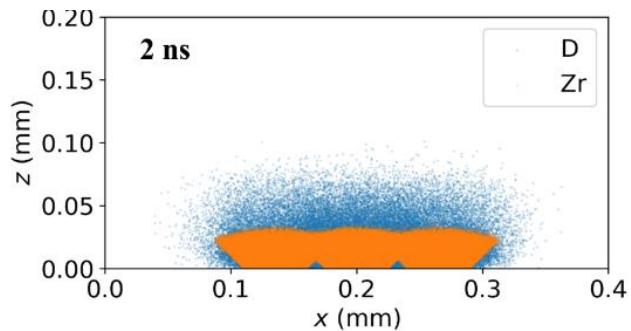
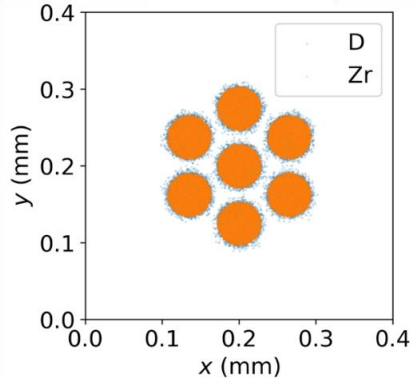
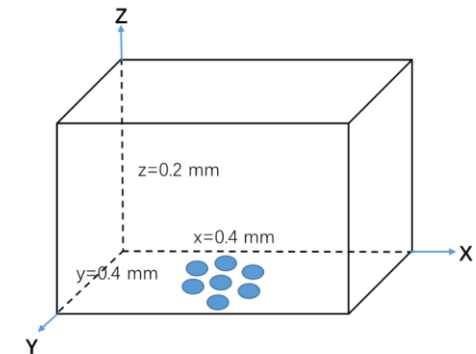
# Ion distribution during plasma expansion of single CS

In the XOZ plane, the distribution of ion density does not differ substantially during plasma expansion of single CS.



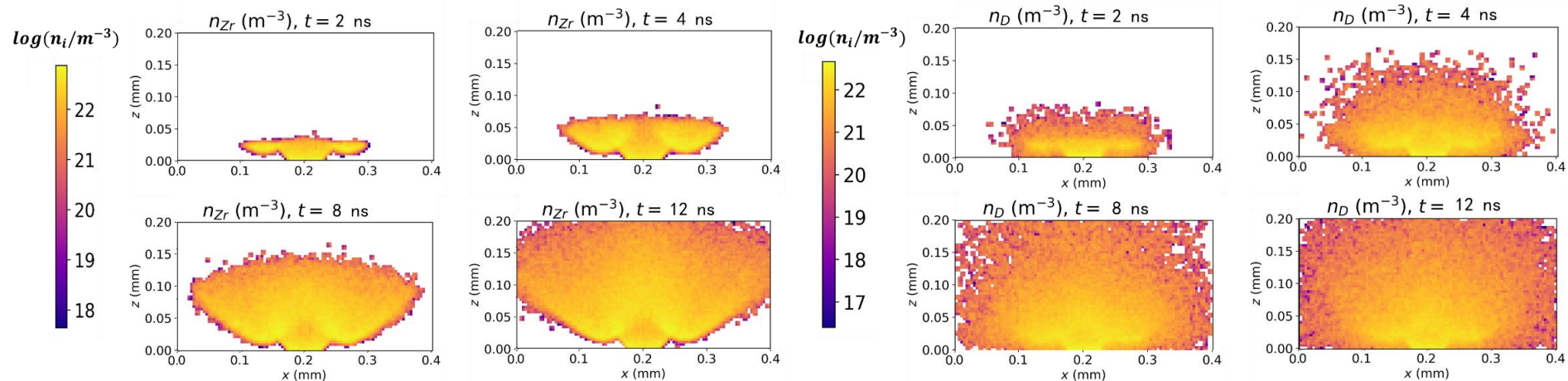
# hybrid simulation on plasma jet mixing of multiply CS

The plasma jets originated from the separate CS **mix together to form a common arc column** after a certain distance from the cathode.



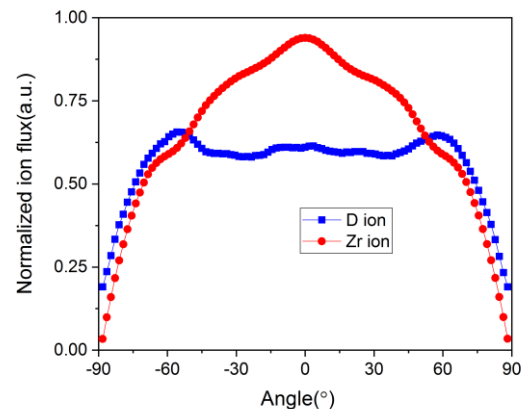
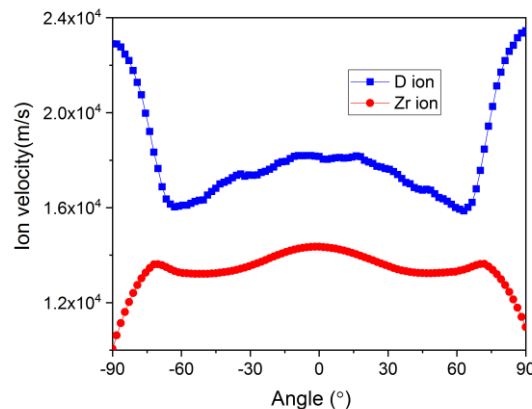
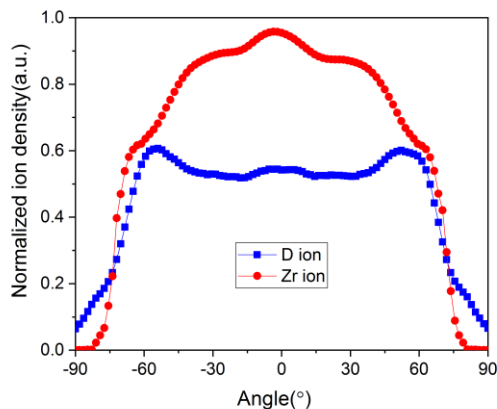
# Ion distribution during plasma jet mixing of multiply CS<sup>32</sup>

In the XOZ plane, the distribution of ion density differs for light ion and heavy ion: heavy ions is more concentrated in the central axis, but light ions are distributed in a much broader area.



# angular distribution of ion density, velocity and flux

- The angular distribution of light and heavy ions is confirmed by **3D hybrid simulation on plasma jet mixing of multiply CS**.
- In the center, the flux of D ions is much smaller than that of Zr; in the edge, the flux of D ions is three times higher than that of Zr.



angular distribution of **ion density (left)**, **velocity (middle)** and **flux (right)**, at a distance 0.16 mm away from the CS

# Table of contents



**Introduction: vacuum arcs of composite electrode**



**Insights from PIC-DSMC simulations**



**Insights from multi-component fluid simulation**



**Recent results of three-dimension hybrid simulation**



**Conclusions**

# Conclusions

---

- ❑ **Regarding multi-component plasma of vacuum arc discharge with composite cathode, we have developed different numerical approaches including fully kinetic particle method, fluid method, and hybrid method.**
- ❑ **During plasma jet mixing, the ion collision is an important factor leading to the separation of light and heavy ions, and three main factors are found: ion mass, ion density and ion temperature.**

**Thank you for listening!**  
**questions or comments?**

